Am J Transl Res 2026;18(8):6612-6626
www.ajtr.org /ISSN:1943-8141/AJTR0173428

Original Article

The role and mechanism of CHST6-mediated lactation modification in lenvatinib resistance in hepatocellular carcinoma cells

Dongdong Wang, Hongqiang Gao, Li Li

The Affiliated Calmette Hospital of Kunming Medical University, The First People's Hospital of Kunming, Kunming, Yunnan, China

Received April 19, 2026; Accepted June 26, 2026; Epub August 15, 2026; Published August 30, 2026

Abstract: Background: Hepatocellular carcinoma (HCC) is the 3rd leading cause of cancer-related death. Approximately 70% of HCC patients present with advanced-stage disease at the time of diagnosis. Lenvatinib is a standard first-line treatment for HCC; however, the development of drug resistance substantially limits its therapeutic efficacy. Methods: Genes associated with lactylation and lenvatinib resistance were identified through bioinformatic analyses. Differentially expressed genes (DEGs) were screened using data from the TCGA-LIHC cohort, the GSE186191 dataset, and a lactylation-related gene datasets. Receiver operating characteristic (ROC) curve analysis, Cox regression analysis, survival analysis, and prognostic evaluation were performed to analyze the association between identified genes and treatment outcomes. After constructing the lenvatinib-resistant MHCC97 cell line (MHCC97-LR) was established, and the effects of CHST6 knockdown on cell viability, apoptosis, cell cycle, lactate content, and the expression of lactylation-related genes were analyzed. Results: A total of 15 overlapping DEGs related to both lactylation and lenvatinib resistance were identified. These genes were involved in multiple metabolic pathways, including lipid and glucose metabolism. CHST6, SPAG4, and PFKFB4 exhibited excellent diagnostic performance for HCC, and their lower expression levels were correlated with favorable prognosis. Cox regression analysis identified CHST6 as the only gene significantly associated with HCC prognosis, demonstrating predictive value for 1-5-year survival in HCC patients. Strikingly, enhanced lactylation was associated with elevated CHST6 expression and greater cell viability in MHCC97-LR cells. Furthermore, CHST6 knockdown reduced the lactate production and the expression of lactylation-associated proteins (Pan-Kla, H3K18la, and H3K56la) in MHCC97-LR cells, along with increased apoptosis and G1-phase cell-cycle arrest in MHCC97-LR cells. Conclusion: CHST6 knockdown reduces intracellular lactate contents and lactylation in MHCC97-LR cells, thereby attenuating lenvatinib resistance and enhancing the antitumor efficacy of lenvatinib in HCC.

Keywords: Hepatocellular carcinoma, lenvatinib resistance, lactylation modification, MHCC97, CHST6

Introduction

Hepatocellular carcinoma (HCC), with cirrhosis as the main risk factor, is a common type of primary liver cancer [1]. HCC accounts for approximately 80% of all liver cancers and was responsible for 747,000 new cases of in 2019, making it the third leading cause of cancer-related deaths worldwide [2-5]. The mortality rate of HCC is close to its incidence, with a median survival of about 6-10 months [6]. Therefore, elucidating the molecular mechanisms underlying HCC progression and identifying novel target are critical for improving targeted therapy and patient survival.

About 70% of HCC patients present with right upper abdominal masses or unexplained disease worsening, indicating advanced disease at the time of diagnosis [7]. Liver transplantation, chemotherapy, and pharmacological therapy remain the mainstay of treatment for HCC patients [8]. Moreover, sorafenib has long been the conventional systemic treatment for HCC; however, it prolongs survival by only about 3 months [9]. Lenvatinib, a multi-targeted tyrosine kinase inhibitor (TKI), demonstrates superior therapeutic efficacy over sorafenib as a first-line agent for advanced HCC [10]. Nevertheless, acquired resistance limits its clinical efficacy [7]. The molecular mechanisms driving

https://doi.org/10.62347/JQSF1666

lenvatinib resistance and strategies to overcome it remain major obstacles to improving therapeutic outcomes.

Recently, lactylation has emerged as a post-translational modification that plays a vital role in regulating cancer cell behavior, shaping tumor microenvironment, and modulating immune responses and immunotherapy [11]. Furthermore, lactylation has been implicated in promoting HCC malignant progression by affecting metabolic proteins [12]. Notably, lenvatinib-resistant HCC cell lines (e.g., Hep3B-LR, Huh7-LR, Hepa1-6-LR) exhibit significantly elevated lactylation levels and higher IC50 values than their parental cells [13]. Therefore, understanding the regulatory mechanisms linking lactylation to lenvatinib resistance could provide new perspectives for targeted therapy and the development of new targets in HCC.

In this study, CHST6 was identified as a differentially expressed gene (DEG) associated with lenvatinib resistance in HCC via bioinformatics analysis. CHST6 activated lactylation in HCC patients and promoted lenvatinib resistance. These findings refine the understanding of lactylation-related mechanisms in lenvatinib resistance and provides a theoretical basis for developing CHST6 as an adjunct target to enhance lenvatinib efficacy in the treatment of HCC.

Methods

Identification of HCC lenvatinib resistance-related genes based on bioinformatics analysis

HCC lenvatinib-resistant cell-related data were extracted from the GEO database, and the GSE186191 dataset [14] was selected for further analysis. The GSE186191 dataset contains RNA-Seq data from two HCC cell lines, Hep3B and Huh7, each containing parental samples (n = 3) and lenvatinib-resistant samples (n = 3). R software (V. 4.2.1) was used for bioinformatics analysis. Briefly, differential expression analysis was performed using the DESeq2 package [15], and DEGs were defined as those with $|\log_2 FC|>1$ and $P<0.05$. Principal component analysis (PCA) was performed on the count matrix to assess sample clustering. Volcano plots were generated for all DEGs, with the top 10 up-regulated and down-regulated DEGs labeled. Expression heatmaps of DEGs were plotted based on the TPM matrix.

Lactylation-related genes (LacGs) were downloaded, and duplicates were removed [16, 17]. The intersection of DEGs from lenvatinib-resistant HCC cells and LacGs yielded 15 shared DEGs. Gene Ontology (GO) and Kyoto Encyclopedia of Genes and Genomes (KEGG) enrichment analyses were performed using the *clusterProfiler* package [18], and protein-protein interaction (PPI) networks were analyzed using *String*. The HCC-related dataset TCGA-LIHC was obtained from the TCGA database, and the expression of 15 shared DEGs was analyzed in normal and tumor populations. The diagnostic and prognostic values of *CHST6*, *SPAG4*, *PFKFB4*, and *EMB* (genes that consistently expressed in Hep3B and Huh7 cells, and clinical datasets), were assessed. Receiver operating characteristic (ROC) curves were plotted using the Python package [19]. Prognostic analyses of CHST6 in TCGA-LIHC dataset were conducted using Log-rank tests and Cox regression with the *survival* package [20]. A nomogram model was constructed and calibrated using the *rms* package [21]. Data visualization was performed using *ggplot2* [22], *rms*, *ggvenn,* and *survminer*.

Establishment of lenvatinib-resistant MHCC97 cells (MHCC97-LR)

MHCC97 cells (MHCC97-H, BNCC359345, BNCC, China) were cultured in high-glucose DMEM (G4515, Servicebio) supplemented with 10% FBS (10099-141, Gibco) and 1% penicillin/streptomycin (15140-122, Gibco) at 37°C in a humidified incubator containing 5% CO_2 (CL-191C, Jingqi, China). Lenvatinib-resistant MHCC97 cells (MHCC97-LR) were constructed according to previously reported methods [23] with minor modifications. Briefly, MHCC97 cells were exposed to 8 μM lenvatinib (S1164, Selleckchem), and the drug concentration was gradually increased in 0.8 μM increments until a final concentration of 40 μM was reached over one week. Cells were maintained at each intermediate concentration for one week before further dose escalation. The constructed MHCC97-LR cells were maintained in medium containing 5 μM lenvatinib for resistance preservation.

Construction and transfection of CHST6 interference plasmid

CHST6 knockdown plasmids were constructed using the pGMLV-SC5 RNAi vector, while CHST6

overexpression plasmids were generated using pCDNA3.1(+) (Genomeditech Co., Ltd.). Briefly, lentiviral packaging and lentiviral titration were performed following plasmid recombination and positive clone sequencing. The siRNA sequences were as follows: sh-NC (TTCTCCGAACGTGTCACGT), sh-CHST6#1 (ATCATATGGTCACTCTATTCAAC), sh-CHST6#2 (TTCGAGAAACCACCAAATTGTTT), sh-CHST6#3 (CTCTTGATTCTTGGTTTTCCTTT), sh-CHST6#4 (GTCTGTACATCACATACATATGC). MHCC97-LR cells were inoculated into 6-well plates at a density of 1×10^5/well. The cell culture medium was replaced with complete medium without P/S, and 4 μL of Lipofectmie 2000 reagent (Invitrogen, USA) was added per well. Transfection was performed by adding 2 μg of either sh-NC or sh-CHST6 plasmid to each well. Cells transfected with sh-NC and sh-CHST6 were designated LR-NC and LR-sh, respectively. After 48 h of incubation, 25 mM sodium lactate (Nala) was added to the medium at 24 h according to the method described in previous researchers [13, 24], generating the Nala, Nala-NC, and Nala-sh groups, respectively.

Cell Counting Kit-8 (CCK-8)

MHCC97 and MHCC97-LR cells were inoculated into 96-well plates at a density of 1×10^4 cells/well and incubated overnight. After treatment with complete medium containing 0, 0.1, 1, 10, and 100 μM lenvatinib for 48 h, 10 μL of CCK-8 (CK04, Dongren Chemistry, China) reagent was added to each well. The plates were incubated for 2 h, and then the absorbance at 450 nm was measured using a microplate reader (EL800, BIO-TEK, USA) to measure cell viability.

Determination of intracellular lactic acid content

Cells were treated according to the instructions of the lactic acid (LA) assay kit (BC2235, Solarbio, USA). After treatment, the supernatant was collected by centrifugation at 12,000 g for 10 min at 4°C. The absorbance of the supernatant was measured at 570 nm using a microplate reader, and the LA content was calculated.

Reverse transcription-quantitative PCR (RT-qPCR)

Total RNA was extracted from cells using TRIZOL lysate (15596026, Lifetech, USA), and RNA concentration was measured using a UV spectrophotometer. cDNA was synthesized using the FastKing RT Kit (With gDNase) (KR116, Tiangen Biochemistry (Beijing) Co., Ltd., China) according to the manufacturer's instructions. Quantitative PCR was subsequently performed using Taq Pro Universal SYBR qPCR Master Mix (Q712-02, Vazyme, China) on a 7500 Real Time PCR System (Applied Biosystems, USA). Relative gene expression levels were calculated using the $2^{-\Delta\Delta Ct}$ method, with GAPDH serving as the internal reference gene. The primer sequences used were as follows: GAPHD: Forward, 5'-TTGCCCTCAACGACCACTTT-3'; Reverse: 5'-TGGTCCAGGGGTCTTACTCC-3'; CHST6: Forward, 5'-TGTGTACTCTGAGGACGA-3'; Reverse: 5'-GATGATGCCCAAGTGAAG-3'; CHST4: Forward, 5'-ATGATTGACAGTCGCATTG-3'; Reverse: 5'-CATCACATAGTAGGGTTGGT-3'.

Western blot

Total cellular proteins were extracted using RIPA lysate (P0013B, Beyotime, China). Protein concentrations were detected using an UV spectrophotometer. Equal amounts of protein (60 μg per lane) were separated by SDS-PAGE electrophoresis and transferred onto PVDF membranes. After blocking with 5% skim milk, the membranes were incubated overnight at 4°C with the following primary antibodies: anti-β-actin (TA-09, Zhongsui Jinqiao, China), anti-CHST6 (ab154332, Abcam, UK), and anti-CHST4 (66623-1-Ig, Proteintech, China). After washing, the membranes were incubated with horseradish peroxidase (HRP)-conjugated secondary antibodies, including goat anti-mouse IgG-HRP (M21001L, Abmart, China) and goat anti-rabbit IgG-HRP (M21002L, Abmart, China), at room temperature for 2 hours. Protein bands were visualized using Immobilon Western Chemiluminescent HRP Substrate (WBKLS0100, Millipore, USA) according to the manufacturer's instructions. Chemiluminescence signals were captured using a Tanon 5200Multi imaging system (Tanon, China).

Flow cytometry

Cell precipitates were collected by centrifugation at 1000 rpm for 5 min. Cell cycle distribution was assessed using the Cell Cycle Assay Kit (C001-200, Seven Seas Bio, China) according to the kit instructions. Briefly, cells were fixed with 1 mL of pre-cooled 70% ethanol for 2

h at 4°C. After fixation, 0.5 mL of propidium iodide (PI) staining solution, prepared in staining buffer (containing 12.5 μL of PI reservoir and 10 μL of RNase A) was added. Cells were incubated in an incubator protected from light for 30 min and then subjected to flow cytometry (VBR, Novocyte advanteon, Agilent, USA) analysis with an excitation wavelength of 488 nm.

Apoptotic cells were detected using the FITC/PI double-staining apoptosis detection kit (A005-4, Seven Seas Bio, China) according to the manufacturer's instructions. Briefly, cells were resuspended in 400 μL banding buffer. Each sample was incubated with 5 μL of FITC dye for 15 min, followed by 10 μL PI for 5 min in the dark. Flow cytometry was performed to detect apoptotic cells. Blank control, FITC single-stained control (5 μL of FITC), and PI single-stained control (10 μL of PI) were used to exclude interference.

Statistical analysis

All experiments were performed with at least three independent replicates. Data were presented as mean ± standard deviation (SD). Comparisons between two groups were performed using Student's t-test. Differences among multiple groups were analyzed using One-way ANOVA followed by Tukey's post hoc test. Statistical analysis and data visualization were performed using GraphPad Prism 9.5. A *P* value of <0.05 was considered statistically significant (ns P>0.05; *P<0.05; **P<0.01; ***P<0.001; ****P<0.0001).

Results

Identification and analysis of DEGs associated with lenvatinib resistance and lactylation in HCC

RNA-seq data from parental and lenvatinib-resistant Hep3B and Huh7 cells were analyzed. Differential expression analysis using the DESeq2 package showed significant gene expression differences between parental and lenvatinib-resistant cells (**Figure 1A**, **1D**). Specifically, 2,815 (1,898 up-regulated and 917 down-regulated) and 2,440 (1229 up-regulated and 1211 down-regulated) DEGs were identified in Hep3B cells and Huh7 cells, respectively (**Figure 1B**, **1C**, **1E**, **1F**).

The intersection of DEGs with lactylation-related genes yielded 15 shared genes (**Figure 1G**). Enrichment analysis indicated that these genes are primarily localized to the nuclear membrane and extracellular matrix, and are associated with glucose and lipid metabolism, platelet-derived growth factor signaling, C2H2 zinc finger motifs, and PPAR signaling pathway (**Figure 1H**, **1I**). In carbohydrate metabolism, ALDOC/PFKFB4 are enriched in fructose and mannose metabolism; ENO2/ALDOC are enriched in glycolysis/gluconeogenesis; and CHST6 is enriched in glycosaminoglycan biosynthesis-chondroitin sulfate (Supplementary Table 1). Further PPI network analysis showed that these DEGs form a functional cluster (**Figure 1J**, **1K**).

Among the 15 DEGs, *CHST6*, *SPAG4*, *PFKFB4*, and *EMB* were consistently elevated in HCC tumors and lenvatinib-resistant HCC cells (**Figure 2A-C**). In ROC curve analysis, *CHST6*, *SPAG4*, and *PFKFB4* demonstrated good diagnostic value for HCC (AUC = 0.814, 0.858, and 0.875, respectively), with sensitivities of 0.5695, 0.6925, and 0.7246, and specificities of 0.96, 0.98, and 0.92, respectively (**Figure 2D**, **2F**).

Based on the optimal cutoff values for *CHST6*, *SPAG4*, *PFKFB4*, and *EMB* derived from ROC analysis, patients were divided into the high- and low- expression groups. Kaplan-Meier survival analysis indicated that high expression of CHST6 (P = 0.040, HR = 2.24, 95% CI 1.38-3.61), SPAG4 (P = 0.013, HR = 2.15, 95% CI 1.42-3.28), and PFKFB4 (P<0.001, HR = 2.92, 95% CI 2.11-4.06) was associated with poorer overall survival. However, for EMB, the log-rank test showed no significant difference (P = 0.587) between patients of high- and low-expression of EMB, suggesting limited prognostic value. Cox regression analysis further confirmed that only CHST6 was independently associated with HCC prognosis (**Figure 2E**).

A nomogram integrating CHST6 expression and clinical features was constructed. The nomogram indicated that *CHST6* contributed more to survival prediction than BMI (**Figure 2G**). Calibration curves showed good predictive performance of the nomogram for 1-5-year survival (**Figure 2H**). These results suggest that *CHST6* has significant prognostic value in HCC and may contribute to the malignant progression of HCC.

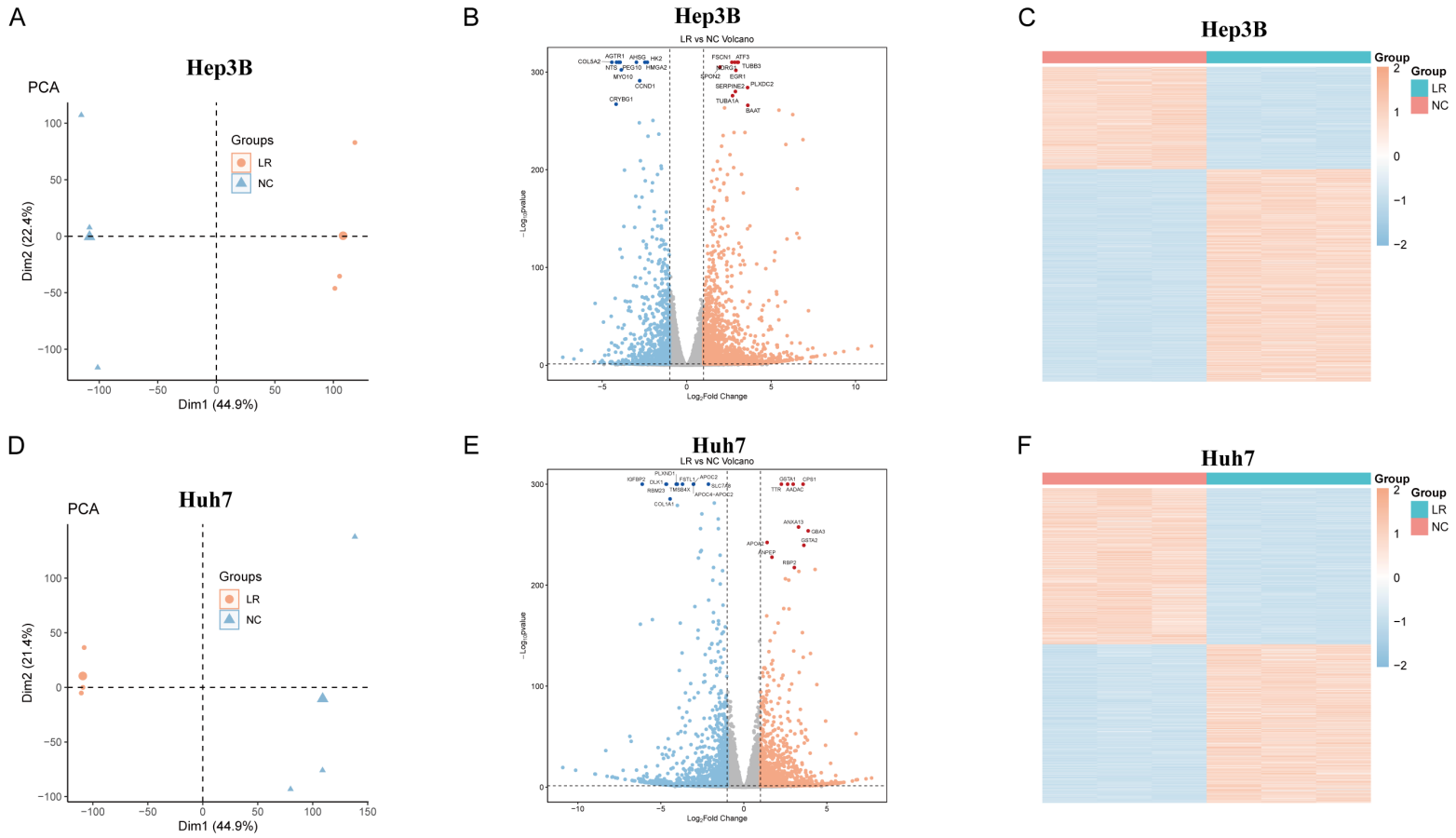
A
Hep3B
PCA
Groups
LR
NC
Dim2 (22.4%)
Dim1 (44.9%)
B
Hep3B
LR vs NC Volcano
−Log10pvalue
Log2Fold Change
C
Hep3B
Group
LR
NC
D
Huh7
PCA
Groups
LR
NC
Dim2 (21.4%)
Dim1 (44.9%)
E
Huh7
LR vs NC Volcano
−Log10pvalue
Log2Fold Change
F
Huh7
Group
LR
NC

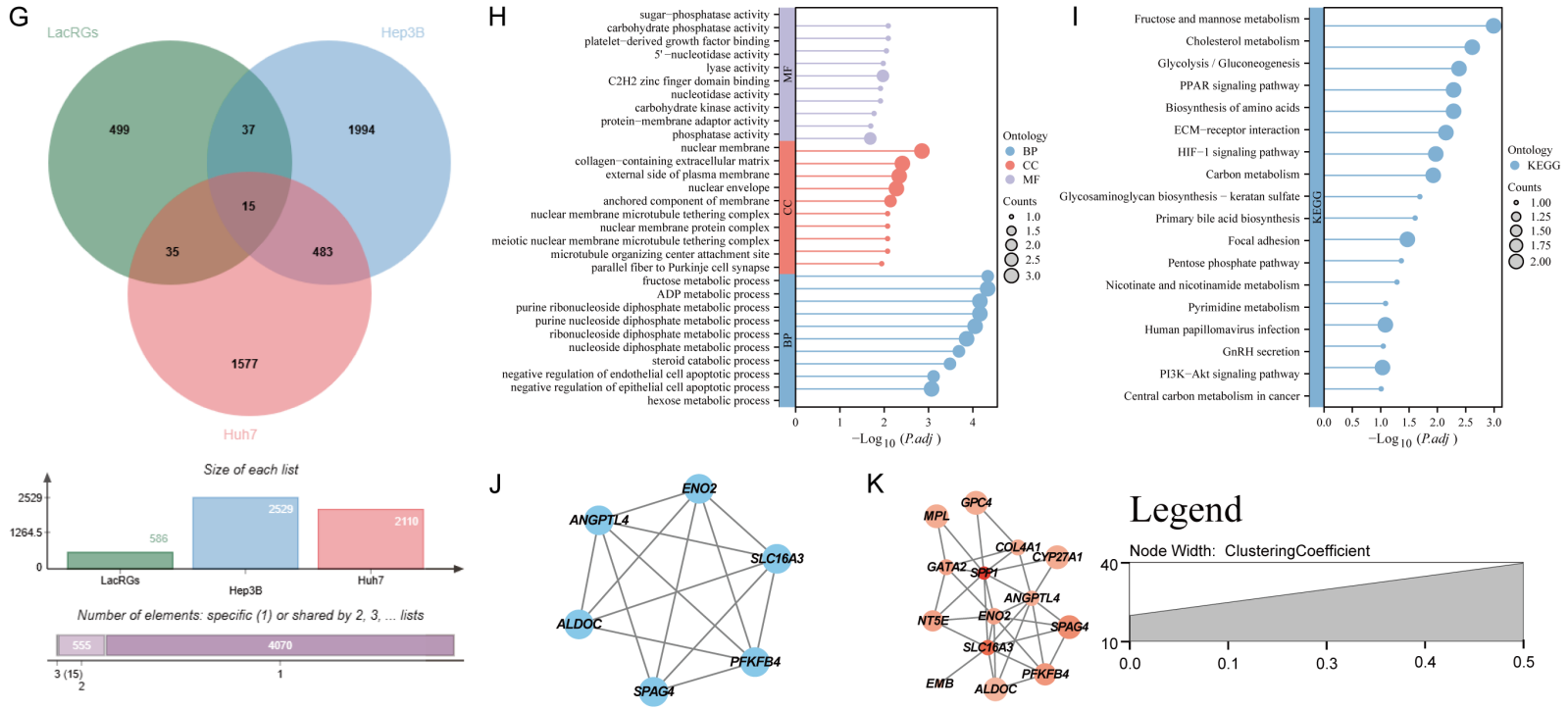

Figure 1. Identification of 15 overlapping DEGs associated with lenvatinib resistance and lactylation in HCC cells. (A-C) Principal component analysis (PCA) plot (A), volcano plot (B), and heatmap (C) showing differential gene expression between lenvatinib-resistant Hep3B cells and parental Hep3B cells; (D-F) PCA plots (D), volcano plots (E), and heat maps (F) showing differential gene expression between lenvatinib-resistant Huh7 cells and parental Huh7 cells; (G) Venn diagram showing the overlap among DEGs identified in the lenvatinib-resistant Hep3B and Huh7 cells and lactylation-related genes; (H, I) GO (H) and KEGG (I) enrichment analyses of the 15 overlapping DEGs; (J, K) Cluster analysis (J) and protein-protein interaction analysis (K) of the 15 overlapping DEGs.

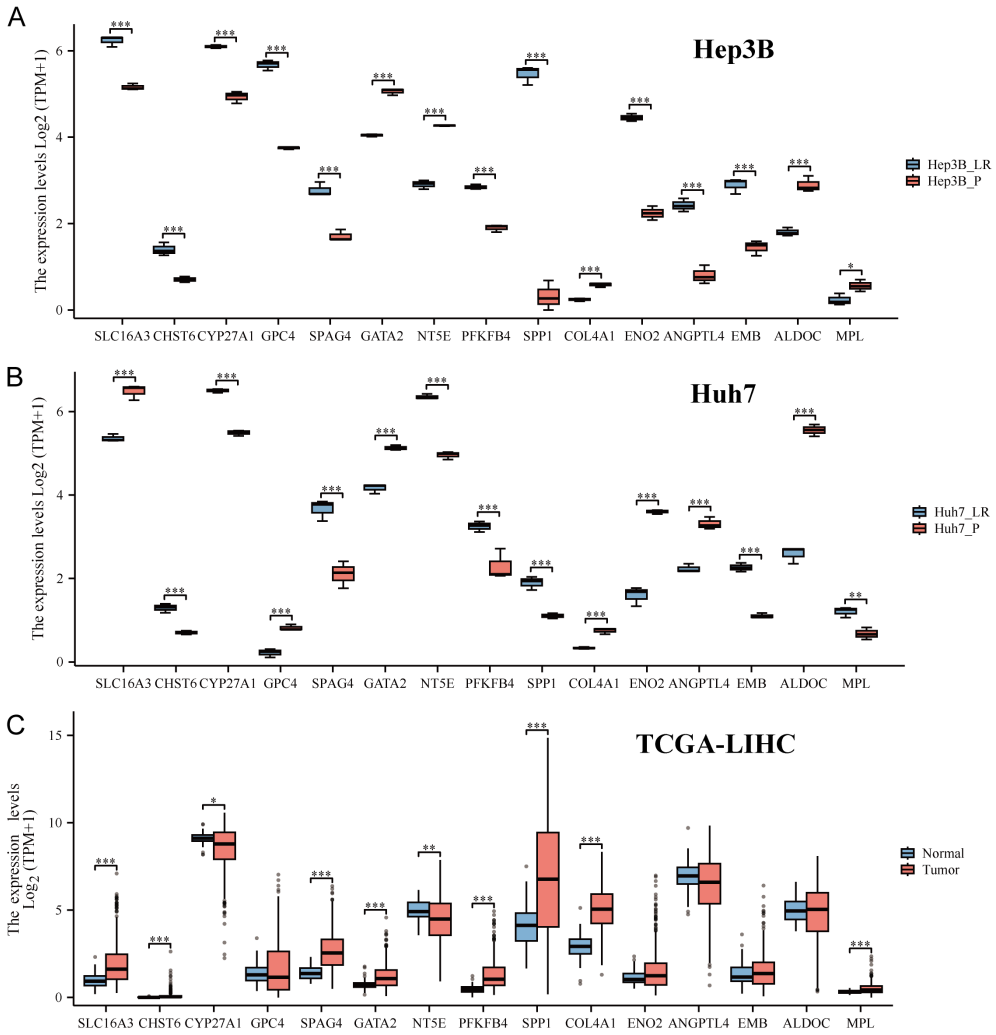

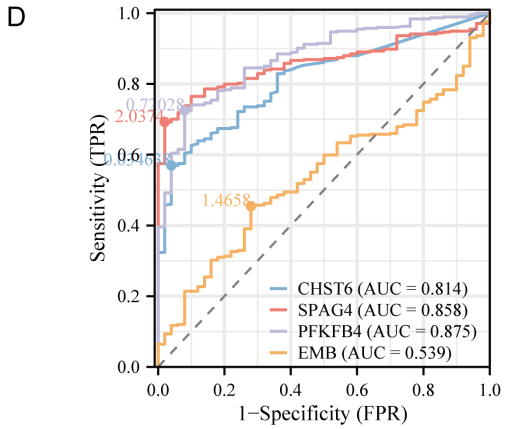

E

Characteristics	Total(N)	Univariate analysis: HR (95% CI)	P value	Total(N)	Multivariate analysis HR (95% CI)	P value
Gender	373			373		
Female	121	Reference		121	Reference	
Male	252	0.793 (0.557 − 1.130)	0.2	252	0.848 (0.491 − 1.467)	0.556
Age	373			373		
<= 60	177	Reference		177	Reference	
> 60	196	1.205 (0.850 − 1.708)	0.295	196	1.321 (0.799 − 2.185)	0.278
BMI	336			336		
<= 25	177	Reference		177	Reference	
> 25	159	0.798 (0.550 − 1.158)	0.235	159	0.548 (0.320 − 0.938)	**0.028**
Pathologic T stage	370			370		
T1	183	Reference		183	Reference	
T2&T3&T4	187	2.126 (1.481 − 3.052)	< 0.001	187	2.107 (1.247 − 3.561)	**0.005**
Pathologic N stage	258			258		
N0	254	Reference		254	Reference	
N1	4	2.029 (0.497 − 8.281)	0.324	4	2.009 (0.451 − 8.953)	0.36
Pathologic M stage	272			272		
M0	268	Reference		268	Reference	
M1	4	4.077 (1.281 − 12.973)	0.017	4	3.233 (0.927 − 11.272)	0.066
PFKFB4	373			373		
Low_PFKFB4	185	Reference		185	Reference	
High_PFKFB4	188	1.243 (0.880 − 1.756)	0.218	188	0.870 (0.528 − 1.433)	0.583
SPAG4	373			373		
Low_SPAG4	187	Reference		187	Reference	
High_SPAG4	186	1.554 (1.099 − 2.197)	0.013	186	1.400 (0.833 − 2.354)	0.204
CHST6	373			373		
Low_CHST6	186	Reference		186	Reference	
High_CHST6	187	1.986 (1.395 − 2.827)	< 0.001	187	2.015 (1.190 − 3.411)	**0.009**
EMB	373			373		
Low_EMB	187	Reference		187	Reference	
High_EMB	186	0.981 (0.694 − 1.385)	0.911	186	0.644 (0.387 − 1.073)	0.091

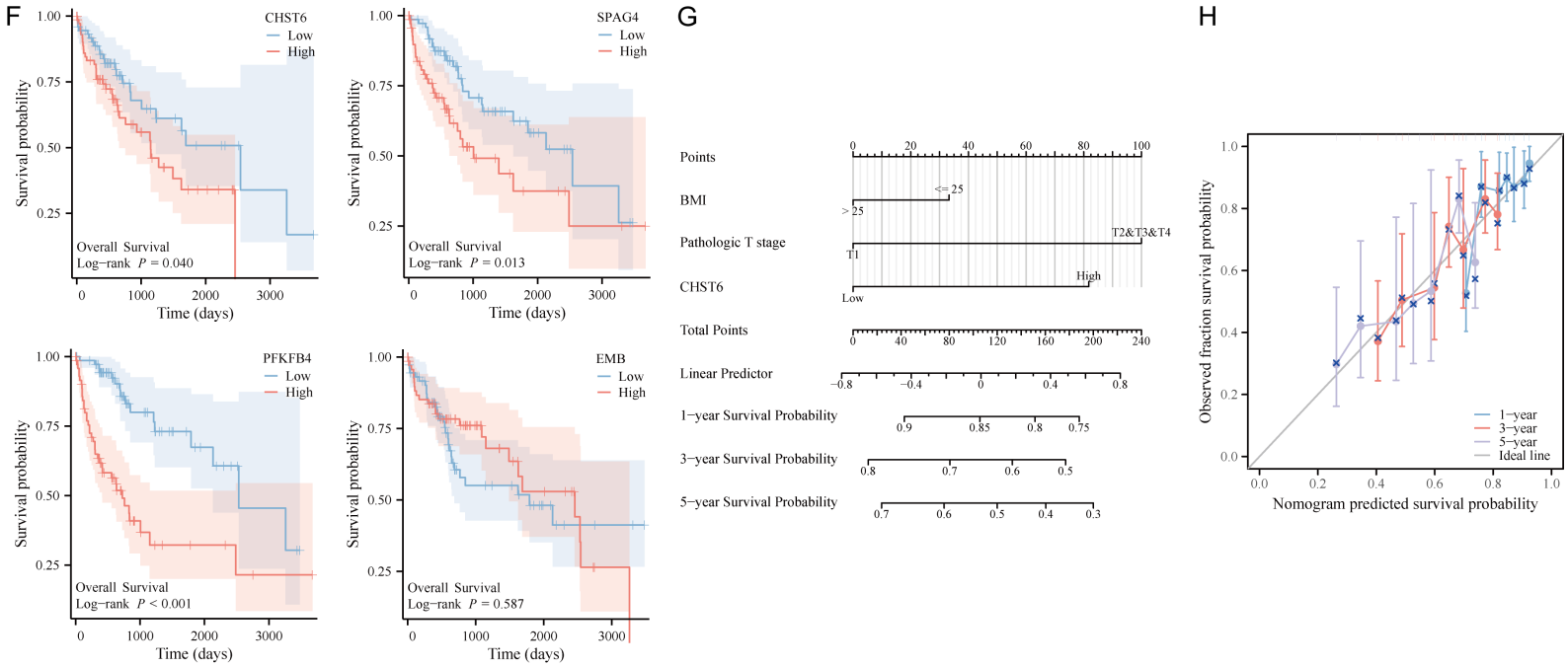

Figure 2. Expression of clinical significance of DEGs related to lactylation and lenvatinib resistance in HCC. (A-C) Expression of the 15 overlapping DEGs in Hep3B (A), Huh7 (B), and TCGA-LIHC (C) datasets; (D) Receiver operating characteristic (ROC) curves assessing the diagnostic performance of *CHST6*, *SPAG4*, *PFKFB4,* and *EMB*; (E) Cox regression analysis of DEGs and clinical variables in the TCGA-LIHC dataset; (F) Kaplan-Meier survival curves showing overall survival stratified by *CHST6*, *SPAG4*, *PFKFB4*, and *EMB* expression; (G, H) Nomograph (G) and calibration curve (H) for predicting 1-5-year overall survival in HCC patients.

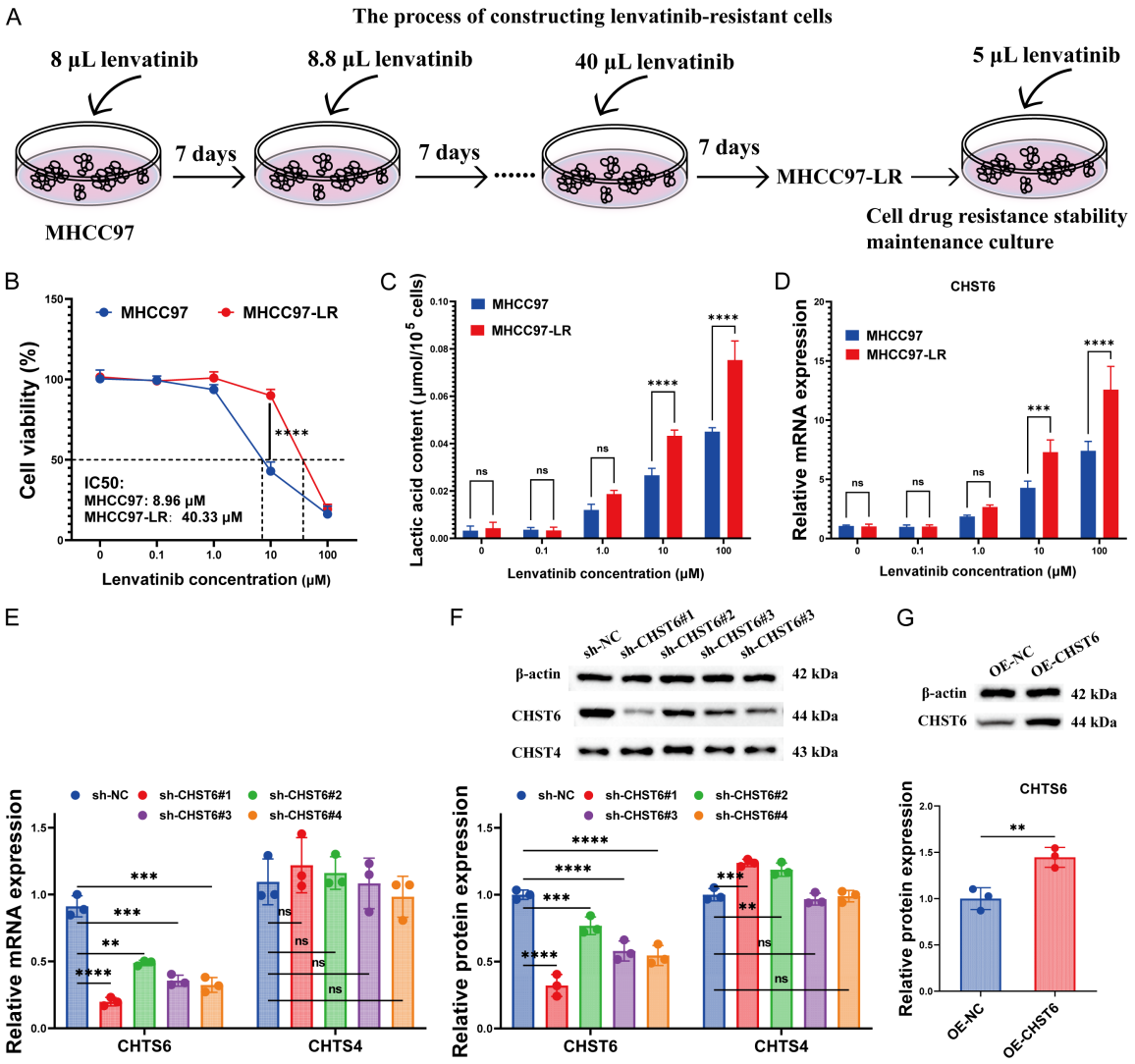

Figure 3. Construction of the lenvatinib-resistant MHCC97-LR cell line and characterization of lactate accumulation and CHST6 expression. (A, B) Schematic diagram of MHCC97-LR construction steps (A) and validation of lenvatinib resistance by cell viability assay (B); (C) Lactate contents in MHCC97 and MHCC97-LR cells following the treatment with 0, 0.1, 1.0, 10, and 100 μM lenvatinib; (D) CHST6 mRNA expression in MHCC97-LR and MHCC97 cells following the treatment with 0, 0.1, 1.0, 10, and 100 μM lenvatinib; (E, F) mRNA (E) and protein (F) expression of CHST6 in MHCC97-LR cells after transfection with CHST6 knockdown plasmid; (G) CHST6 protein expression in MHCC97-LR cells after transfection with CHST6 overexpression plasmid. ns indicates no significant difference; **, ***, **** represent $P<0.01$, $P<0.001$, and $P<0.0001$, respectively.

Elevated lactylation and CHST6 expression in MHCC97 lenvatinib-resistant cells

The MHCC97-LR cell line was established by exposure of parental MHCC97 cells to increasing concentrations of lenvatinib (**Figure 3A**). The IC50 of MHCC97-LR was increased by approximately 4.5 times compared to parental MHCC97 cells (**Figure 3B**), confirming acquired drug resistance. Notably, treatment with 10 μM and 100 μM of lenvatinib significantly increased CHST6 expression and lactate content in MHCC97-LR cells compared with parental MHCC97 cells (**Figure 3C**, **3D**), suggesting that CHST6 and lactylation are implicated in lenvatinib resistance.

For the CHST6 knockdown, sh-CHST6#1 demonstrated the most effective efficiency (**Figure 3E**, **3F**). Additionally, sh-CHST6#4 served as an off-target control for sh-CHST6#1 in subsequent studies. To further evaluate off-tar-

get effects, CHST4, a homolog of CHST6, was examined. Neither sh-CHST6#1 nor sh-CHST6#4 significantly altered CHST4 mRNA expression (**Figure 3E**). At the protein level, sh-CHST6#1 promoted CHST4 protein expression, whereas sh-CHST6#4 had no significant effect on CHST6 protein expression (**Figure 3F**). These results indicate that using both sh-CHST6#1 and sh-CHST6#4 minimizes off-target interference. Furthermore, an overexpression control group for CHST6 (OE-CHST6) was established to validate the functional impact of CHST6 on MHCC97-LR cell behavior (**Figure 3G**).

CHST6 promoted MHCC97-LR malignant phenotype

Transfection of sh-CHST6 and OE-CHST6 into MHCC97-LR cells successfully modulated CHST6 expression (**Figure 4A**). CHST6 knockdown resulted in decreased viability (**Figure 4B**), increased apoptosis (**Figure 4C**), and G1 phase cell cycle arrest (**Figure 4D**) in MHCC97-LR cells. These results indicate that CHST6 contributes to the malignant phenotype of lenvatinib-resistant MHCC97-LR cells. Furthermore, treatment with Nala to induce lactylation enhanced both CHST6 expression and cell viability in MHCC97-LR cells, demonstrating that lactylation promotes malignant phenotype of MHCC97-LR cells. Furthermore, under conditions of elevated lactylation, CHST6 knockdown resulted in reduced cell viability, increased apoptosis, and cell arrest in G1 phases (**Figure 4A-D**). Notably, both sh-CHST6#1 and sh-CHST6#4 exerted consistent effects, whereas CHST6 overexpression exerted the opposite regulatory pattern (**Figure 4**). These findings suggest that CHST6 inhibition may serve as a potential therapeutic strategy for HCC treatment.

CHST6 promoted MHCC97-LR lactonization

CHST6 knockdown significantly reduced lactate content in MHCC97-LR cells (**Figure 5A**). Consistently, the expression levels of lactylation-associated proteins, including Pan-Kla, H3K18la, and H3K56la, were significantly reduced following CHST6 knockdown (**Figure 5B-D**).

To further investigate the relationship between CHST6 and lactylation, MHCC97-LR cells were treated with sodium lactate (Nala) to induce lactylation. Treatment with Nala significantly increased intracellular lactate content and the expression of lactylation-associated proteins, including Pan-Kla, H3K18la, and H3K56la, in MHCC97-LR cells. Notably, CHST6 knockdown effectively attenuated these Nala-induced effects (**Figure 5A-D**).

Furthermore, sh-CHST6#1 and sh-CHST6#4 produced comparable regulatory effects, whereas CHST6 overexpression demonstrated the opposite pattern to that of CHST6 knockdown, leading to increased lactate levels and elevated expression of lactylation-related proteins (**Figure 5**). These findings suggest that CHST6 inhibition may attenuate lenvatinib resistance in HCC through suppression of lactylation.

Discussion

The liver plays a central role in tyrosine metabolism and gluconeogenesis. Studies have demonstrated that tyrosine metabolism is dysregulated in HCC patients, characterized by reduced tyrosine aminotransferase and increased tyrosine [25, 26]. Lenvatinib, an oral multi-target TKI, has emerged as a first-line drug for the treatment of unresectable HCC [27]. It exerts anti-tumor effects primarily through inhibition of multiple receptor tyrosine kinases, including vascular endothelial growth factor receptor (VEGFR) and fibroblast growth factor receptor (FGFR), thereby suppressing tumor angiogenesis and proliferation.

Despite its clinical efficacy, the development of drug resistance significantly limits the long-term benefits of lenvatinib treatment. Previous studies have shown that long-term use of lenvatinib may induce over-activation of VEGFR-related signaling pathways and structural changes in FGFR kinase domains, ultimately reducing drug-targeted binding efficiency and therapeutic responsiveness [28].

CHST6, also known as carbohydrate sulfotransferase 6, is located on chromosome 16q23.1 and encodes a sulfotransferase belonging to the CHST family [29, 30]. The CHST family members participate in sulfation modification of glycosaminoglycans by catalyzing the transfer of sulfate groups to carbohydrates [31]. Current studies have mostly associated CHST6 with macular corneal dystrophy [32, 33]. In con-

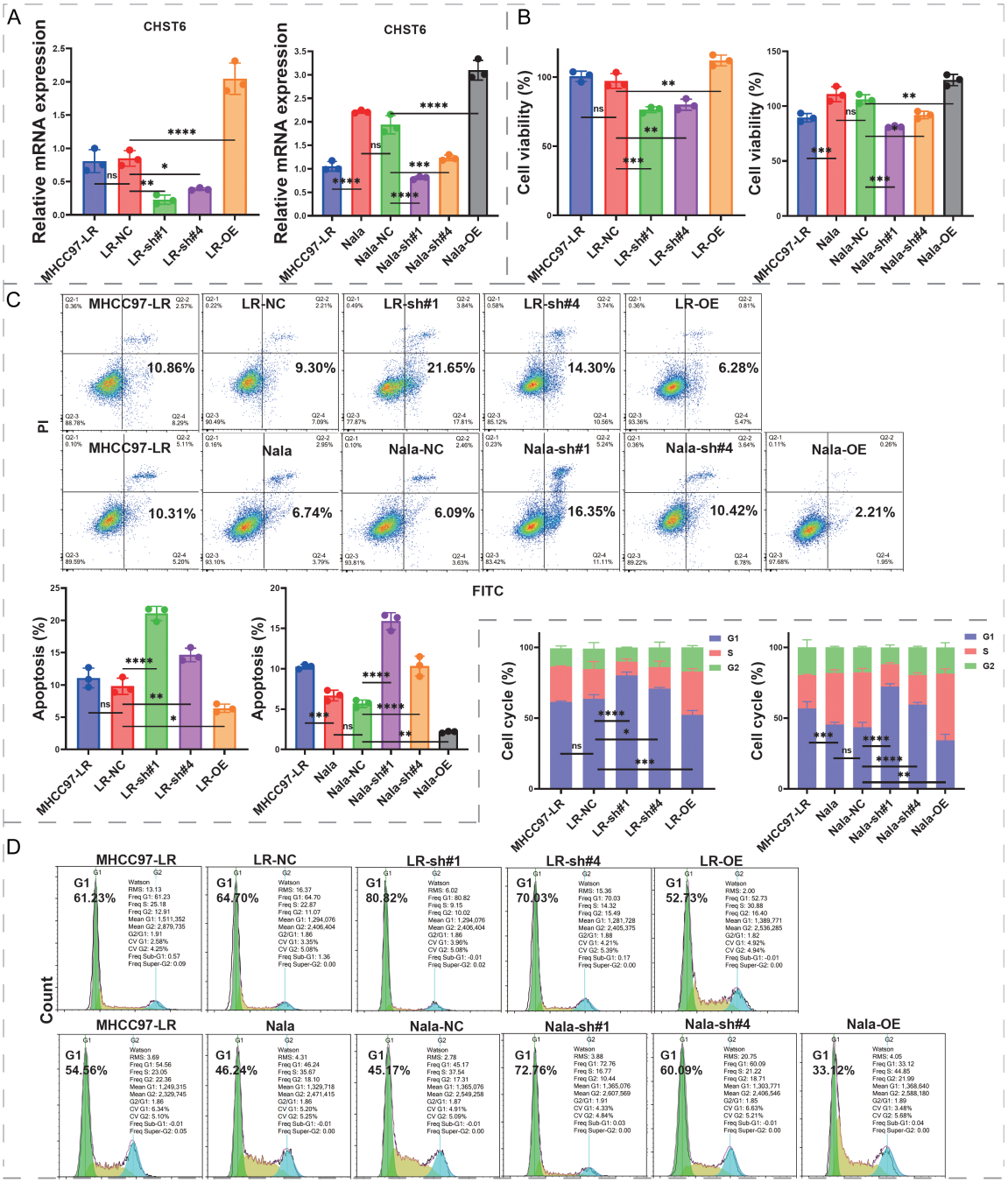

Figure 4. Effect of CHST6 knockdown on the malignant phenotype of MHCC97-LR cells. A: mRNA expression of CHST6 in MHCC97-LR cells under normal and lactylation-induced conditions; B: Effects of CHST6 knockdown on MHCC97-LR cell viability as detected by CCK-8; C: Effects of CHST6 knockdown on MHCC97-LR cell apoptosis detected by flow cytometry; D: Effects of CHST6 knockdown on MHCC97-LR cell cycle distribution detected by flow cytometry. ns indicates no significant difference; *, **, ***, **** represent $P<0.05$, $P<0.01$, $P<0.001$, and $P<0.0001$, respectively.

trast, CHST4 has been reported to inhibit hepatitis B virus-associated HCC progression and serve as a prognostic predictor in HCC [34]. Unlike previous studies, this study identified CHST6 as gene associated with lenvatinib resistance and prognosis in HCC, demonstrating its potential as a good predictor of patient survival.

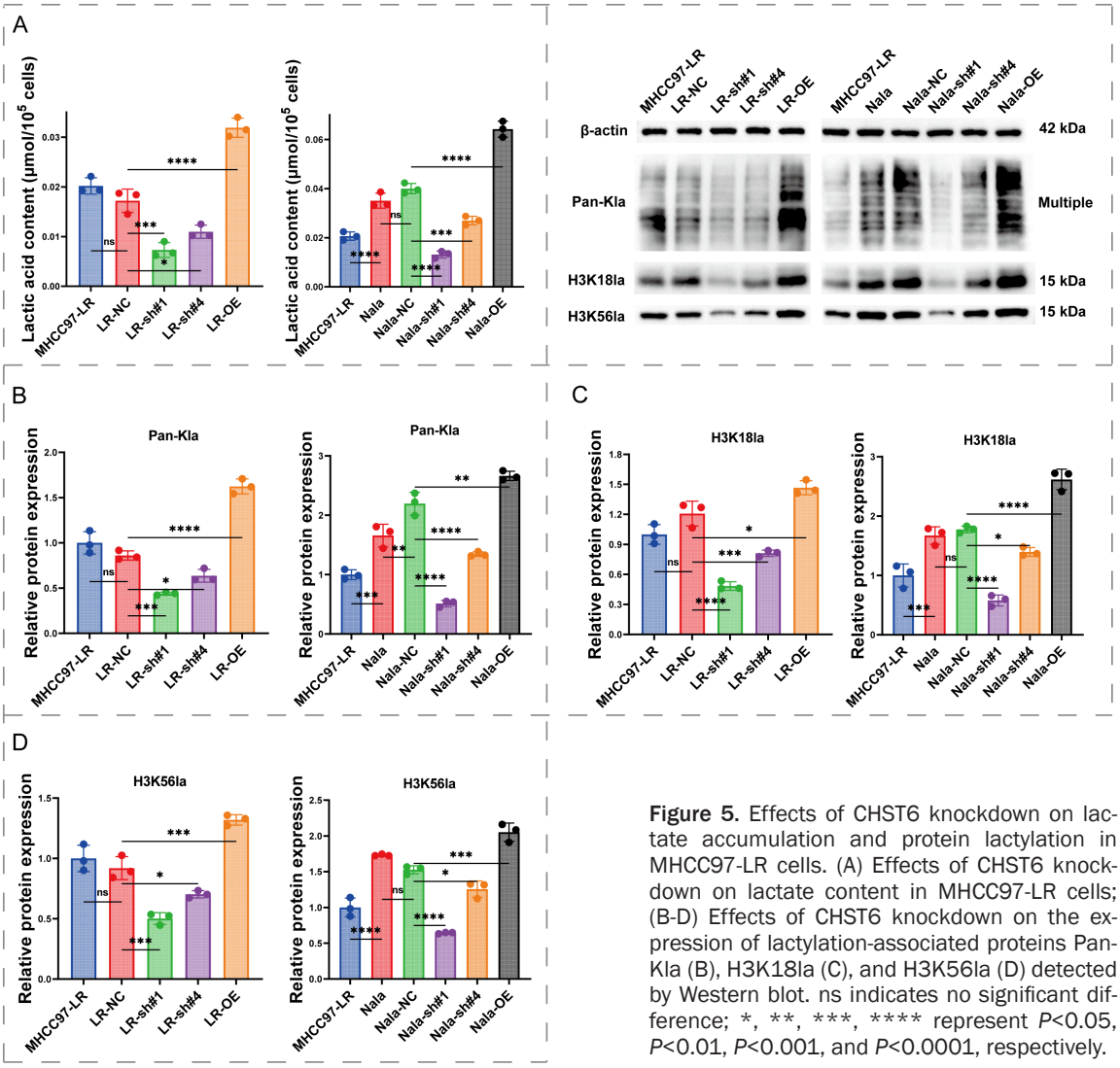

Figure 5. Effects of CHST6 knockdown on lactate accumulation and protein lactylation in MHCC97-LR cells. (A) Effects of CHST6 knockdown on lactate content in MHCC97-LR cells; (B-D) Effects of CHST6 knockdown on the expression of lactylation-associated proteins Pan-Kla (B), H3K18la (C), and H3K56la (D) detected by Western blot. ns indicates no significant difference; *, **, ***, **** represent $P<0.05$, $P<0.01$, $P<0.001$, and $P<0.0001$, respectively.

Notably, HCC progression leads to increased lactate accumulation and extracellular acidification, which disrupt the immune microenvironment and promote malignant behaviors [35]. Consistently, we observed elevated lactate content in HCC cells, which were further increased in lenvatinib-resistant MHCC97-LR cells. Additionally, CHST6 has been implicated in the Warburg effect (aerobic glycolysis) in multiple cancers, including thyroid cancer [36], endometrial cancer [37], clear cell renal cell carcinoma [38], and low-grade gliomas [39]. This metabolic reprogramming contributes to lactate-induced suppression of anticancer immune cells caused by glucose over-conversion in a wide range of cancer cells [40, 41].

Notably, this study found that CHST6 is involved in the KEGG pathway "glycosaminoglycan biosynthesis - keratan sulfate". Previous studies have demonstrated that CHPF2 mediates chondroitin sulfate synthesis to promote HCC progression [42], and that heparan sulfate proteoglycan GPC3 is overexpressed in HCC but undetectable in normal liver [43]. These findings suggest a potential link between CHST6-mediated sulfated glycosaminoglycan synthesis and HCC progression. Moreover, dysregulation of lactate metabolism has also been associated with the development of liver disease [44]. Notably, it was reported that β-hydroxybutyrate can modulate lactylation to reverse sorafenib resistance. Similarly, in our study, CHST6 knockdown in MHCC97-LR cells resulted in decreased lactate levels and reduced expression of lactylation-associated proteins, including Pan-Kla, H3K18la, and H3K56la. Furthermore, it was found that the

hypoxia-associated factor (HIF-1) may mediate metabolic reprogramming of HCC resistance, particularly lactonization, to overcome sorafenib resistance in hypoxic HCC [45]. This is similar to our findings that CHST6 knockdown decreased cell viability, increased apoptosis, and induced G1-phase cell-cycle arrest in MHCC97-LR cells, consistent with previous reports that genistein and swainsonine inhibit HCC cell proliferation via G1-phase blockade [46, 47]. These findings suggest that CHST6 may contribute to lenvatinib resistance by regulating lactate accumulation and protein lactylation. Mechanistically, CHST6 knockdown may inhibit lenvatinib resistance by interfering with sulfation of histones (e.g., H3Y99sulf) or kinases associated with Warburg effect or hypoxia-mediated reprogramming [48, 49]. However, this inference requires further validation.

In summary, our study identified CHST6 as a gene associated with HCC survival and lenvatinib resistance through bioinformatics analysis. Reduced CHST6 expression decreased lactate contents and the expression of lactylation-associated proteins, leading to cell-cycle arrest and increased apoptosis in MHCC97-LR cells. These findings illustrate that CHST6 knockdown counteracts lenvatinib resistance in HCC by inhibiting lactylation. It is important to mention that our results were validated *in vitro*, and further in vivo and clinical experiments (e.g., analyzing CHST6 expression in patient samples before and after lenvatinib treatment) are needed to support the translational relevance of CHST6 as a therapeutic target. Moreover, validation should be conducted in diverse HCC cell models to confirm the generalizability of our results. Furthermore, the hypothesis that CHST6 regulates the Warburg effect or hypoxia-related pathways lacks supporting experimental data and warrants further experimental investigation. Future studies should elucidate how CHST6 regulates lactate production, identify upstream regulators and downstream effectors, and characterize specific, functionally relevant non-histone targets relevant to its function. Investigating whether exogenous lactate supplementation can reverse the sensitizing effect of CHST6 knockdown on lenvatinib efficacy would further strengthen the mechanistic understanding.

Conclusion

CHST6 expression and intracellular lactate levels were significantly elevated in lenvatinib-resistant MHCC97-LR cells. CHST6 knockdown reduced lactate accumulation and protein lactylation, along with increased apoptosis and G1-phase cell-cycle arrest. In summary, CHST6 contributes to lenvatinib resistance through the regulation of lactylation and that inhibition of CHST6 may enhance the sensitivity of HCC cells to lenvatinib by attenuating lactylation-associated resistance mechanisms.

Acknowledgements

We thank the TCGA and GEO databases and the corresponding contributors. This study was supported by the National Key Clinical Specialty Construction Project (China).

Disclosure of conflict of interest

None.

Address correspondence to: Li Li, Department of Hepato-Biliary-Pancreatic Surgery, The Affiliated Calmette Hospital of Kunming Medical University, The First People's Hospital of Kunming, No. 504 Qingnian Road, Kunming 650100, Yunnan, China. E-mail: kmll6d@163.com

References

[1] Ganesan P and Kulik LM. Hepatocellular carcinoma: new developments. Clin Liver Dis 2023; 27: 85-102.

[2] GBD 2019 Diseases and Injuries Collaborators. Global burden of 369 diseases and injuries in 204 countries and territories, 1990-2019: a systematic analysis for the global burden of disease study 2019. Lancet 2020; 396: 1204-1222.

[3] Chrysavgis L, Giannakodimos I, Diamantopoulou P and Cholongitas E. Non-alcoholic fatty liver disease and hepatocellular carcinoma: clinical challenges of an intriguing link. World J Gastroenterol 2022; 28: 310-331.

[4] Sung H, Ferlay J, Siegel RL, Laversanne M, Soerjomataram I, Jemal A and Bray F. Global cancer statistics 2020: GLOBOCAN estimates of incidence and mortality worldwide for 36 cancers in 185 countries. CA Cancer J Clin 2021; 71: 209-249.

[5] Brar G, Greten TF, Graubard BI, McNeel TS, Petrick JL, McGlynn KA and Altekruse SF. Hepatocellular carcinoma survival by etiology: a seer-medicare database analysis. Hepatol Commun 2020; 4: 1541-1551.

[6] Goutté N, Sogni P, Bendersky N, Barbare JC, Falissard B and Farges O. Geographical variations in incidence, management and survival of hepatocellular carcinoma in a western country. J Hepatol 2017; 66: 537-544.
[7] Qin Y, Han S, Yu Y, Qi D, Ran M, Yang M, Liu Y, Li Y, Lu L, Liu Y and Li Y. Lenvatinib in hepatocellular carcinoma: resistance mechanisms and strategies for improved efficacy. Liver Int 2024; 44: 1808-1831.
[8] Mazzaferro V, Regalia E, Doci R, Andreola S, Pulvirenti A, Bozzetti F, Montalto F, Ammatuna M, Morabito A and Gennari L. Liver transplantation for the treatment of small hepatocellular carcinomas in patients with cirrhosis. N Engl J Med 1996; 334: 693-699.
[9] Llovet JM, Ricci S, Mazzaferro V, Hilgard P, Gane E, Blanc JF, de Oliveira AC, Santoro A, Raoul JL, Forner A, Schwartz M, Porta C, Zeuzem S, Bolondi L, Greten TF, Galle PR, Seitz JF, Borbath I, Häussinger D, Giannaris T, Shan M, Moscovici M, Voliotis D and Bruix J; SHARP Investigators Study Group. Sorafenib in advanced hepatocellular carcinoma. N Engl J Med 2008; 359: 378-390.
[10] Zhao Y, Zhang YN, Wang KT and Chen L. Lenvatinib for hepatocellular carcinoma: from preclinical mechanisms to anti-cancer therapy. Biochim Biophys Acta Rev Cancer 2020; 1874: 188391.
[11] Chen J, Huang Z, Chen Y, Tian H, Chai P, Shen Y, Yao Y, Xu S, Ge S and Jia R. Lactate and lactylation in cancer. Signal Transduct Target Ther 2025; 10: 38.
[12] Kotsiliti E. Lactylation and HCC progression. Nat Rev Gastroenterol Hepatol 2023; 20: 131.
[13] Lu Y, Zhu J, Zhang Y, Li W, Xiong Y, Fan Y, Wu Y, Zhao J, Shang C, Liang H and Zhang W. Lactylation-driven IGF2BP3-mediated serine metabolism reprogramming and RNA m6A-modification promotes lenvatinib resistance in HCC. Adv Sci (Weinh) 2024; 11: e2401399.
[14] Hou W, Bridgeman B, Malnassy G, Ding X, Cotler SJ, Dhanarajan A and Qiu W. Integrin subunit beta 8 contributes to lenvatinib resistance in HCC. Hepatol Commun 2022; 6: 1786-1802.
[15] Liu S, Wang Z, Zhu R, Wang F, Cheng Y and Liu Y. Three differential expression analysis methods for RNA sequencing: limma, EdgeR, DESeq2. J Vis Exp 2021; 175: e62528.
[16] Peng T, Sun F, Yang JC, Cai MH, Huai MX, Pan JX, Zhang FY and Xu LM. Novel lactylation-related signature to predict prognosis for pancreatic adenocarcinoma. World J Gastroenterol 2024; 30: 2575-2602.
[17] Huang A, Sun Z, Hong H, Yang Y, Chen J, Gao Z and Gu J. Novel hypoxia- and lactate metabolism-related molecular subtyping and prognostic signature for colorectal cancer. J Transl Med 2024; 22: 587.
[18] Wu T, Hu E, Xu S, Chen M, Guo P, Dai Z, Feng T, Zhou L, Tang W, Zhan L, Fu X, Liu S, Bo X and Yu G. clusterProfiler 4.0: a universal enrichment tool for interpreting omics data. Innovation (Camb) 2021; 2: 100141.
[19] Kui B, Pintér J, Molontay R, Nagy M, Farkas N, Gede N, Vincze Á, Bajor J, Gódi S, Czimmer J, Szabó I, Illés A, Sarlós P, Hágendorn R, Pár G, Papp M, Vitális Z, Kovács G, Fehér E, Földi I, Izbéki F, Gajdán L, Fejes R, Németh BC, Török I, Farkas H, Mickevicius A, Sallinen V, Galeev S, Ramírez-Maldonado E, Párniczky A, Erőss B, Hegyi PJ, Márta K, Váncsa S, Sutton R, Szatmary P, Latawiec D, Halloran C, de-Madaria E, Pando E, Alberti P, Gómez-Jurado MJ, Tantau A, Szentesi A and Hegyi P; Hungarian Pancreatic Study Group. EASY-APP: an artificial intelligence model and application for early and easy prediction of severity in acute pancreatitis. Clin Transl Med 2022; 12: e842.
[20] Therneau T and Grambsch P. Modeling survival data: extending the Cox model. 2000.
[21] Eng KH, Schiller E and Morrell K. On representing the prognostic value of continuous gene expression biomarkers with the restricted mean survival curve. Oncotarget 2015; 6: 36308-36318.
[22] Gustavsson EK, Zhang D, Reynolds RH, Garcia-Ruiz S and Ryten M. ggtranscript: an R package for the visualization and interpretation of transcript isoforms using ggplot2. Bioinformatics 2022; 38: 3844-3846.
[23] Liu X, Gao X, Yang Y, Yang D, Guo Q, Li L, Liu S, Cong W, Lu S, Hou L, Wang B and Li N. EVA1A reverses lenvatinib resistance in hepatocellular carcinoma through regulating PI3K/AKT/p53 signaling axis. Apoptosis 2024; 29: 1161-1184.
[24] Duan W, Liu W, Xia S, Zhou Y, Tang M, Xu M, Lin M, Li X and Wang Q. Warburg effect enhanced by AKR1B10 promotes acquired resistance to pemetrexed in lung cancer-derived brain metastasis. J Transl Med 2023; 21: 547.
[25] Watanabe A, Higashi T, Sakata T and Nagashima H. Serum amino acid levels in patients with hepatocellular carcinoma. Cancer 1984; 54: 1875-1882.
[26] Fu L, Dong SS, Xie YW, Tai LS, Chen L, Kong KL, Man K, Xie D, Li Y, Cheng Y, Tao Q and Guan XY. Down-regulation of tyrosine aminotransferase at a frequently deleted region 16q22 contributes to the pathogenesis of hepatocellular carcinoma. Hepatology 2010; 51: 1624-1634.
[27] Chen P, Li Y, Wei P, Liang L, Li B, Cao Y, Han X, Wang Y, Duan X, Jia H, Zhao T and Ren J. siRNA targeting PD-L1 delivered with attenuated Salmonella enhanced the anti-tumor ef-

fect of lenvatinib on mice bearing Hepatocellular carcinoma. Int Immunopharmacol 2022; 111: 109127.
[28] Al-Salama ZT, Syed YY and Scott LJ. Lenvatinib: a review in hepatocellular carcinoma. Drugs 2019; 79: 665-674.
[29] Vance JM, Jonasson F, Lennon F, Sarrica J, Damji KF, Stauffer J, Pericak-Vance MA and Klintworth GK. Linkage of a gene for macular corneal dystrophy to chromosome 16. Am J Hum Genet 1996; 58: 757-762.
[30] Akama TO, Nishida K, Nakayama J, Watanabe H, Ozaki K, Nakamura T, Dota A, Kawasaki S, Inoue Y, Maeda N, Yamamoto S, Fujiwara T, Thonar EJ, Shimomura Y, Kinoshita S, Tanigami A and Fukuda MN. Macular corneal dystrophy type I and type II are caused by distinct mutations in a new sulphotransferase gene. Nat Genet 2000; 26: 237-241.
[31] Klaassen CD and Boles JW. Sulfation and sulfotransferases 5: the importance of 3'-phosphoadenosine 5'-phosphosulfate (PAPS) in the regulation of sulfation. FASEB J 1997; 11: 404-418.
[32] Hao XD, Liu YN, Hu SH, Pan XJ and Chen P. Association of macular corneal dystrophy with excessive cell senescence and apoptosis induced by the novel mutant CHST6. Exp Eye Res 2022; 214: 108862.
[33] Sultana A, Sridhar MS, Klintworth GK, Balasubramanian D and Kannabiran C. Allelic heterogeneity of the carbohydrate sulfotransferase-6 gene in patients with macular corneal dystrophy. Clin Genet 2005; 68: 454-460.
[34] Zhang L, Fan Y, Wang X, Yang M, Wu X, Huang W, Lan J, Liao L, Huang W, Yuan L, Pan H, Wu Y, Chen L and Guan J. Carbohydrate sulfotransferase 4 inhibits the progression of hepatitis B virus-related hepatocellular carcinoma and is a potential prognostic marker in several tumors. Front Oncol 2020; 10: 554331.
[35] Peng X, He Z, Yuan D, Liu Z and Rong P. Lactic acid: the culprit behind the immunosuppressive microenvironment in hepatocellular carcinoma. Biochim Biophys Acta Rev Cancer 2024; 1879: 189164.
[36] Xu F, Xu H, Li Z, Huang Y, Huang X, Li Y, Zheng X, Chen Y and Lin L. Glycolysis-based genes are potential biomarkers in thyroid cancer. Front Oncol 2021; 11: 534838.
[37] Wang ZH, Zhang YZ, Wang YS and Ma XX. Identification of novel cell glycolysis related gene signature predicting survival in patients with endometrial cancer. Cancer Cell Int 2019; 19: 296.
[38] Xing Q, Zeng T, Liu S, Cheng H, Ma L and Wang Y. A novel 10 glycolysis-related genes signature could predict overall survival for clear cell renal cell carcinoma. BMC Cancer 2021; 21: 381.
[39] Liu G, Lu Y, Gao D, Huang Z and Ma L. Identification of an energy metabolism-related six-gene signature for distinguishing and forecasting the prognosis of low-grade gliomas. Ann Transl Med 2023; 11: 146.
[40] Jeong H, Kim S, Hong BJ, Lee CJ, Kim YE, Bok S, Oh JM, Gwak SH, Yoo MY, Lee MS, Chung SJ, Defrêne J, Tessier P, Pelletier M, Jeon H, Roh TY, Kim B, Kim KH, Ju JH, Kim S, Lee YJ, Kim DW, Kim IH, Kim HJ, Park JW, Lee YS, Lee JS, Cheon GJ, Weissman IL, Chung DH, Jeon YK and Ahn GO. Tumor-associated macrophages enhance tumor hypoxia and aerobic glycolysis. Cancer Res 2019; 79: 795-806.
[41] Husain Z, Huang Y, Seth P and Sukhatme VP. Tumor-derived lactate modifies antitumor immune response: effect on myeloid-derived suppressor cells and NK cells. J Immunol 2013; 191: 1486-1495.
[42] Liang Z, Ye Y, Deng Z, Lan H, Liu C, Xu Y, Fan M, Liu Z, Wu P, An L and Wang C. CHPF2 as a novel biomarker and ponicidin as a potential therapeutic agent in hepatocellular carcinoma. Pharmacol Res 2025; 215: 107698.
[43] Xiao X, Huang Q, Lin X, Zahid KR, Huang X, Liu T and Zeng T. Current methods for the detection of glypican-3. Anal Methods 2024; 16: 152-160.
[44] Yao S, Chai H, Tao T, Zhang L, Yang X, Li X, Yi Z, Wang Y, An J, Wen G, Jin H and Tuo B. Role of lactate and lactate metabolism in liver diseases (Review). Int J Mol Med 2024; 54: 59.
[45] Bao MH and Wong CC. Hypoxia, metabolic reprogramming, and drug resistance in liver cancer. Cells 2021; 10: 1715.
[46] Gu Y, Zhu CF, Dai YL, Zhong Q and Sun B. Inhibitory effects of genistein on metastasis of human hepatocellular carcinoma. World J Gastroenterol 2009; 15: 4952-4957.
[47] You N, Liu W, Wang T, Ji R, Wang X, Gong Z, Dou K and Tao K. Swainsonine inhibits growth and potentiates the cytotoxic effect of paclitaxel in hepatocellular carcinoma in vitro and in vivo. Oncol Rep 2012; 28: 2091-2100.
[48] Yu W, Zhou R, Li N, Lei ZC, Guo D, Peng F, Li Y, Bai X, Feng S, Wang Y, He J, Yin S, Zeng X, He L, Gao Y, Li M, Guo YR, Liu K and Wang Y. Histone tyrosine sulfation by SULT1B1 regulates H4R3me2a and gene transcription. Nat Chem Biol 2023; 19: 855-864.
[49] Li F, Si W, Xia L, Yin D, Wei T, Tao M, Cui X, Yang J, Hong T and Wei R. Positive feedback regulation between glycolysis and histone lactylation drives oncogenesis in pancreatic ductal adenocarcinoma. Mol Cancer 2024; 23: 90.

Supplementary Table 1. KEGG enrichment analysis of differentially expressed genes

ONTOLOGY	ID	Description	q-value	Gene ID
KEGG	hsa00051	Fructose and mannose metabolism	0.02146654	*ALDOC/PFKFB4*
KEGG	hsa04979	Cholesterol metabolism	0.02180346	*ANGPTL4/CYP27A1*
KEGG	hsa00010	Glycolysis/Gluconeogenesis	0.02180346	*ENO2/ALDOC*
KEGG	hsa01230	Biosynthesis of amino acids	0.02180346	*ENO2/ALDOC*
KEGG	hsa03320	PPAR signaling pathway	0.02180346	*ANGPTL4/CYP27A1*
KEGG	hsa04512	ECM-receptor interaction	0.02479956	*COL4A1/SPP1*
KEGG	hsa04066	HIF-1 signaling pathway	0.03115562	*ENO2/ALDOC*
KEGG	hsa01200	Carbon metabolism	0.03115562	*ENO2/ALDOC*
KEGG	hsa00533	Glycosaminoglycan biosynthesis - keratan sulfate	0.04771645	*CHST6*
KEGG	hsa00120	Primary bile acid biosynthesis	0.05204214	*CYP27A1*
KEGG	hsa04510	Focal adhesion	0.06477445	*COL4A1/SPP1*
KEGG	hsa00030	Pentose phosphate pathway	0.07586702	*ALDOC*
KEGG	hsa00760	Nicotinate and nicotinamide metabolism	0.08369969	*NT5E*
KEGG	hsa00240	Pyrimidine metabolism	0.11489794	*NT5E*
KEGG	hsa05165	Human papillomavirus infection	0.11489794	*COL4A1/SPP1*
KEGG	hsa04929	GnRH secretion	0.11489794	*SPP1*
KEGG	hsa04151	PI3K-Akt signaling pathway	0.11489794	*COL4A1/SPP1*
KEGG	hsa05230	Central carbon metabolism in cancer	0.11489794	*SLC16A3*